



Innate immune humoral factors, C1q and factor H, with differential pattern recognition properties, alter macrophage response to carbon nanotubes

Kirsten M. Pondman, PhD^{a,b}, Lina Pednekar, PhD^a, Basudev Paudyal, MSc^a,
Anthony G. Tsolaki, DPhil^a, Lubna Kouser, BSc^a, Haseeb A. Khan, PhD^c,
Mohamed H. Shamji, PhD^{d,e}, Bennie ten Haken, PhD^b, Gudrun Stenbeck, PhD^a,
Robert B. Sim, DPhil^{f,g}, Uday Kishore, PhD^{a,*}

^aCentre for Infection, Immunity and Disease Mechanisms, Department of Life Sciences, College of Health and Life Sciences, Brunel University London, UK

^bNeuro Imaging, MIRA Institute, University of Twente, Enschede, the Netherlands

^cDepartment of Biochemistry, College of Science, King Saud University, Riyadh, Saudi Arabia

^dAllergy and Clinical Immunology, National Heart and Lung Institute, Imperial College London, London, UK

^eMRC & Asthma UK Centre in Allergic Mechanisms of Asthma, London, UK

^fDepartment of Pharmacology, University of Oxford, Oxford, UK

^gDepartment of Infection, Immunity and Inflammation, University of Leicester, Leicester, UK

Received 5 March 2015; accepted 21 June 2015

Abstract

Interaction between the complement system and carbon nanotubes (CNTs) can modify their intended biomedical applications. Pristine and derivatised CNTs can activate complement primarily via the classical pathway which enhances uptake of CNTs and suppresses pro-inflammatory response by immune cells. Here, we report that the interaction of C1q, the classical pathway recognition molecule, with CNTs involves charge pattern and classical pathway activation that is partly inhibited by factor H, a complement regulator. C1q and its globular modules, but not factor H, enhanced uptake of CNTs by macrophages and modulated the pro-inflammatory immune response. Thus, soluble complement factors can interact differentially with CNTs and alter the immune response even without complement activation. Coating CNTs with recombinant C1q globular heads offers a novel way of controlling classical pathway activation in nanotherapeutics. Surprisingly, the globular heads also enhance clearance by phagocytes and down-regulate inflammation, suggesting unexpected complexity in receptor interaction.

From the Clinical Editor: Carbon nanotubes (CNTs) maybe useful in the clinical setting as targeting drug carriers. However, it is also well known that they can interact and activate the complement system, which may have a negative impact on the applicability of CNTs. In this study, the authors functionalized multi-walled CNT (MWNT), and investigated the interaction with the complement pathway. These studies are important so as to gain further understanding of the underlying mechanism in preparation for future use of CNTs in the clinical setting.

© 2015 The Authors. Published by Elsevier Inc. This is an open access article under the CC BY-NC-ND license (<http://creativecommons.org/licenses/by-nc-nd/4.0/>).

Key words: Carbon nanotubes; Nanotherapeutics; Immune system; Innate immunity; Complement; C1q; Factor H

A rapid recognition and clearance of nanoparticles including carbon nanotubes (CNTs) from the systemic circulation by the immune system can seriously undermine the intended application of nanoparticles as intravenous drug delivery platforms.¹ Therefore, understanding how nanoparticles interact with

cellular and humoral immune components is essential for their strategic and specific *in vivo* use.^{1–6}

The innate immune system plays a key role in the recognition and clearance of pathogens, altered-self, and synthetic particles including nanoparticles.^{1,3,6–8} The complement system is one of the key innate immune mechanisms and is activated through three pathways. The classical pathway is initiated by C1q, a charge pattern recognition protein consisting of 18 chains (6A, 6B and 6C) each composed of an N-terminal collagen domain (cC1q) and a C-terminal globular head (gC1q) domain. These polypeptides assemble to form a structure of 6 heterotrimeric globular heads, linked together by the collagen regions. C1q most notably binds to IgG and IgM-bearing immune complexes

Disclosures: L.P., A.G.T., L.K., G.S. and U.K. thank Brunel University London for strategic Infrastructure funding. H.A.K. acknowledges the Deanship of Scientific Research at King Saud University for funding via Group No. RGP-009.

*Corresponding author.

E-mail addresses: uday.kishore@brunel.ac.uk, ukishore@hotmail.com (U. Kishore).

<http://dx.doi.org/10.1016/j.nano.2015.06.009>

1549-9634/© 2015 The Authors. Published by Elsevier Inc. This is an open access article under the CC BY-NC-ND license (<http://creativecommons.org/licenses/by-nc-nd/4.0/>).

through its gC1q domains, but can also bind charge clusters/hydrophobic patches on self, non-self and altered-self targets.^{9,10} C1q binding to its targets activates proteases C1r and C1s, which are bound to the cC1q domain, and C1s activates C4 and C2 forming C4b2a (a C3 convertase) which activates C3, forming C3a and C3b, of which the latter can bind to the target surface. C3b and its breakdown products iC3b and C3d interact with C3 receptors on phagocytic cells.¹⁰ C3b also binds to C4b2a, forming C4b2a3b, a protease that can bind and activate C5, and ultimately drives formation of C5b-9 (the membrane attack complex; MAC), which forms a channel in membranes, lysing cells.¹⁰ In the lectin pathway, binding of MBL or ficolins to targets via vicinal-diols or acetyl-groups on sugars activates MASPs, leading to C4 and C2 activation.¹⁰ In the alternative pathway, hydrolysis of a thiol-ester in C3 to form C3(H₂O) results in formation of a complex with factor B, which is cleaved by factor D, to form C3(H₂O)Bb (a homologue of C4b2a). C3(H₂O)Bb activates C3, to form C3a and C3b, which can bind covalently to surfaces. Surface-bound C3b then interacts with factor B and factor D to yield C3 convertase (C3bBb). C3bBb, an unstable protease, can be stabilized by properdin to form C3bBbP. Factor H (FH) regulates the alternative pathway by binding to C3b, inhibiting interaction with factor B, and then factor I, a regulatory protease, cleaves C3b in the C3b-FH complex to form iC3b, a potent opsonin, which is unable to form C3bBb.^{10–12} Like C1q, FH binds to targets mainly via interactions with charge clusters, and thus competes with C1q for binding to some targets, thereby also inhibiting classical pathway activation.^{11,13}

Pristine and functionalized CNTs activate complement, mainly through the classical pathway, and to a minor extent through the alternative^{3,4,6,8,14–18} and the lectin pathways.^{4,19,20} Complement activation by CNTs offers an intriguing challenge since C3b-opsonized CNTs can be cleared via complement receptors on phagocytes²¹ prior to reaching the targeted tissue for drug delivery. Complement by-products (C3a, C4a, and C5a) are potent anaphylatoxins, and can induce inflammation and hypersensitivity reactions.^{3,8,10} MAC formation can potentially cause damage to cells and tissues in close vicinity of complement-activating nanoparticles.⁶ Classical pathway-activating CNTs get internalized more efficiently by macrophages, leading to down-regulation of pro-inflammatory cytokines.²¹ However, Au–Ni nanowires of similar dimensions activate complement very poorly, causing reduced phagocytosis and increased pro-inflammatory response by immune cells.²² Complement deposition can potentially sequester CNTs away from PAMP-PRR engagement on immune cell surfaces, and dampen inflammation via up-regulation of anti-inflammatory IL-10.²²

Surface modifications of hydrophobic CNTs are essential to disperse them in aqueous media that can be achieved by covalent or non-covalent surface coating. Non-covalent adsorption of dispersants (proteins, polymers and nucleic acids) onto the CNT surface does not alter their structure. Covalent functionalization alters their walls by making small defects, commonly via oxidation, leading to carboxyl groups on the surface.²³ Here, we functionalized a type of pristine multi-walled CNT (MWNT), covalently by oxidation (Ox-MWNT), or non-covalently with carboxymethyl-cellulose (CMC-MWNT), each having carboxyl

functional groups. Given that CNTs (pristine or functionalized) offer repetitive recognition patterns of polarity and hydrophobicity, we examined the nature of interaction of C1q, the first recognition subcomponent of the classical pathway, with Ox-MWNT and CMC-MWNT. We also included FH in the study, a competitive inhibitor of C1q for certain ligands, which can act as a regulator of classical as well as alternative pathway.²⁴ Both C1q and FH, which can be locally synthesised during immune cell activation, can have functions without involving complement activation.²⁵ Here, we show differential interaction of C1q and FH with CNTs, which can impact upon complement activation, phagocytosis, and immune response.

Methods and materials

Dispersion of MWNTs by non-covalent and covalent functionalization

MWNTs were purchased from Arry Nano, Germany with an outer diameter of 10–20 nm and a length of 5–20 μm. Non-covalent functionalization was achieved by 2 min sonication in PBS in 2:1 mass ratio with CMC (Sigma), followed by centrifugation at 8000g to remove clusters, washing in PBS, and filtration of excess CMC using a 0.2 μm filter (Whatman). For covalent functionalization, a modified procedure described by Li et al²³ was used. 100 mg of pristine MWNTs was added to a 50 ml mixture of H₂SO₄ (10 M) and HNO₃ (10 M) in 3:1 ratio, sonicated in a water-bath (RT for 1 h), and then probe-sonicated for 30 min (50% ON, 50% OFF) on ice, in order to exfoliate the MWNTs and homogenize the dispersion. After being refluxed at 120 °C for 48 h, the resulting mixture of Ox-MWNTs, after being cooled down and diluted with distilled water, was centrifuged at 11,000g for 30 min. Water was added to the pellets to re-suspend Ox-MWNTs and then centrifuged three times. The amorphous carbon due to the partial oxidation of the outer structure was removed by stirring the Ox-MWNTs in 10 mM NaOH overnight.²⁶ The dispersion was then filtered through a 0.1 μm filter, followed by extensive washing in water in order to remove NaOH. Ox-MWNTs were dialyzed against distilled water and washed in PBS.

Purification of C1q and factor H from human plasma

C1q and FH were purified from human plasma as described previously.¹³

Recombinant human C1q globular head modules (ghA, ghB and ghC) and substitution mutants

The ghA, ghB and ghC modules and their substitution mutants (Arg^{A162}Ala/Glu, Arg^{B114}Gln/Glu, His^{B117}Asp, Arg^{B129}Ala/Glu, Lys^{B136}Glu, Arg^{B163}Ala/Glu, Tyr^{B175}Leu, His^{C101}Ala, Arg^{C156}Glu, Lys^{C170}Glu) were expressed as fusion proteins linked to maltose binding protein (MBP) in *Escherichia coli* BL21 and purified using amylose resin.^{27–29} These mutants were selected based on earlier data showing their involvement in C1q binding to a range of ligands including IgG, IgM, CRP and PTX3. LPS was removed using Polymyxin B agarose gel (Sigma) and its level was determined by Limulus amoebocyte lysate assay (BioWhittaker, USA) (~4 pg μg⁻¹ for ghA and ghB; ~5 pg μg⁻¹ for ghC).

Coating of CNTs with C1q, ghA, ghB, ghC and FH

C1q, ghA, ghB, ghC, substitution mutants and FH were incubated overnight (2:1 weight ratio) with CMC-MWNT or Ox-MWNT in affinity buffer (50 mM Tris-HCl, pH 7.5, 150 mM NaCl, 5 mM CaCl₂) and unbound proteins were washed away by repeated centrifugation at 17,000g for 10 min. Protein binding was analyzed by SDS-PAGE under reduced conditions. A range of protein:CNT weight ratios was analyzed (1:2, 1:1, 2:1, 4:1 and 8:1) and 2:1 ratio was found to be optimal.

Complement consumption and hemolytic assays for the classical pathway

A complement consumption assay was performed as described earlier⁶ to examine modulation of the classical pathway activation by protein-coated CNTs. Samples of coated and uncoated CMC-MWNT and Ox-MWNT (100 µg/ml in affinity buffer) were incubated with occasional shaking at 37 °C for 1 h with an equal volume of human serum 1:1 diluted in dextrose gelatin veronal buffer (DGVB⁺⁺; 2.5 mM sodium barbital, 71 mM NaCl, 0.15 mM CaCl₂, 0.5 mM MgCl₂, 2.5% w/v glucose, 0.1% w/v gelatin, pH7.4). This was followed by centrifugation (13,000g, 10 min), and the collected supernatants were tested for their complement activity by measuring the capacity to lyse antibody-sensitized sheep erythrocytes (EA; Ref. ⁶). 100 µl of EA cells (1 × 10⁸ cells/ml in DGVB⁺⁺) were added to serial dilutions (100 µl) of each supernatant in DGVB⁺⁺ and incubated for 1 h at 37 °C. Following centrifugation (5000 rpm, 5 min), 100 µl of the supernatant was collected and released hemoglobin was measured at 405 nm. Total hemolysis (100%) was measured by lysing EA with water. Background spontaneous hemolysis (0%) was determined by incubating EA with buffer (DGVB⁺⁺) only. Serum diluted identically but without CNTs was used as positive control.

Biotinylation of CNTs

CMC-MWNT and Ox-MWNT were dialyzed into 0.1 M MES buffer, pH 5 and their concentration adjusted to 0.2 mg/ml. Pentylamine biotin (Pierce; 2 mg) was added to 2 ml of CMC-MWNT or Ox-MWNT and 20 µl of a 20 mg/ml solution of *N*-(3-dimethylaminopropyl)-*N'*-ethylcarbodiimide hydrochloride (EDC, Sigma) was added and incubated at RT for 2 h with stirring, and then biotinylation was stopped by adding 100 µl of 0.1 M ethanolamine pH 8.2 (Sigma). The resulting biotin-CMC-MWNT and biotin-Ox-MWNT were dialyzed against PBS in order to remove residual reactants and MES.

Phagocytosis assay

U937 cells (a monocytic cell line derived from histiocytic lymphoma) were cultured in complete RPMI-1640 (GIBCO) containing 10% fetal calf serum (FCS), 2 mM L-glutamine, 100 U/ml penicillin, 100 µg/ml streptomycin and 1 mM sodium pyruvate (all from Sigma), and passaged and washed in AIM-V Albumax serum free medium (GIBCO) before use. In each well of a 24 well plate, 5 × 10⁵ cells were seeded in AIM-V AlbuMAX serum free medium with supplements but no FCS.

Twenty micrograms of biotin-CMC-CNT or biotin-Ox-MWNTs coated with C1q, factor H, ghA, ghB or ghC was added to each well and incubated for 6 h. Cells were harvested and washed 5 times in PBS (centrifugation at 300g) and stored at –80 °C until further use. All experiments were performed in duplicate.

For quantification of phagocytosis,²¹ 25 µl lysis buffer (10 mM HEPES, 20 mM NaCl, 0.5 mM EDTA, 1% w/v Triton X 100) was added to the cell pellets. After cell lysis, 25 µl of 0.1 mg/ml horse IgG (MRC ICU, Oxford) in PBS was added (as a blocking agent) to the dispersion. Microtitre wells (NUNC, polysorb) were coated with 100 µl Avidin (Pierce) at 50 µg/ml in 0.1 M Na₂CO₃, pH 9.0 for 1 h at RT, followed by blocking with 1 mg/ml horse IgG in PBS for 1 h at RT. Next, 50 µl of a solution or cell lysate containing biotin-CMC-MWNT or biotin-Ox-MWNT and 50 µl of 0.1 mg/ml horse IgG was incubated for 1 h in each well. The plate was washed 7 times with 0.1 mg/ml horse IgG in PBS to remove excess CNTs and then incubated with 1:2000 Streptavidin-HRP (Sigma) for 1 h at RT. TMB (Biolegend, UK) was used as a substrate for HRP and the yellow product was read at 450 nm.

Isolation of human macrophages and fluorescence microscopy

CMC-MWNTs were suspended in 0.1 M MES, pH 5 and labeled with AlexaFluor488-cadaverine (Invitrogen) for 2 h at RT in a 2:1 mass ratio in the presence of 1 mM EDC. Labeled CMC-MWCNTs were recovered by centrifugation (10,000g, 10 min) and washed 3 times with PBS to remove unincorporated label. Purified proteins were incubated overnight at a 2:1 mass ratio with AlexaFluor488-cadaverine labeled CMC-MWNT in affinity buffer at 4 °C with agitation. Excess protein was removed by washing twice with PBS. Treated AlexaFluor488-cadaverine labeled CMC-MWNTs were recovered by centrifugation and dispersed in PBS in a water bath sonicator.

The uptake of protein-treated and untreated, fluorescently-labeled CMC-MWNT was examined using monocyte-derived human macrophages as described in Ref. ²². Human PBMCs (1 × 10⁶) were seeded on 13 mm diameter cover slips and incubated for 14 days at 37 °C, 5% CO₂ in a humidified atmosphere. Mature macrophages were exposed to 4 µg/ml protein-treated or untreated AlexaFluor488-cadaverine labeled CMC-MWCNTs in 500 µl of serum-free medium for 3 h. Cells were washed twice with PBS, fixed with 4% formaldehyde for 10 min, washed twice, and processed for immunofluorescence. The coverslips were stained for 30 min with 1.6 µM Hoechst 33342 and 2 µg/ml Alexa-Fluor546-conjugated wheat germ agglutinin (Invitrogen). Cells were then washed twice, mounted using Citifluor anti-fade (Citifluor, UK) and observed with a Zeiss 780 confocal microscope with 40× oil-lens using ZEN software (Zeiss, UK).

Quantitative PCR analysis for cytokine mRNA expression

In a 24-well plate, 10 µg of protein-coated CMC-MWNTs or Ox-MWNTs in 500 µl of PBS were added to each well containing 5 × 10⁵ U937 cells in AIM-V Albumax serum-free medium and incubated for 15, 30, 45, 60, 120 or 360 min inside a 5% CO₂–95% air incubator at 37 °C (PBS only for 30 min as control). Cells were harvested and spun down (3000g, 5 min) and stored at –80 °C. Total RNA was extracted from frozen cell

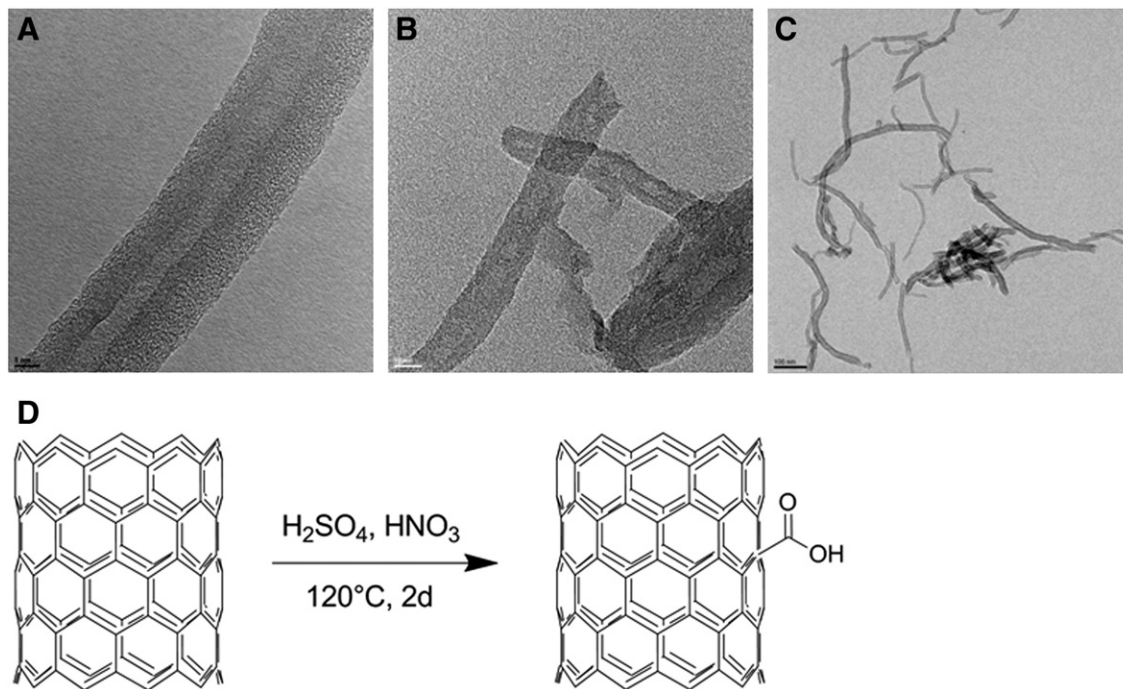


Figure 1. (a) High resolution TEM image of pristine MWNT showing a high number of undamaged parallel carbon walls. The external diameter is ~22 nm while the inner diameter of the CNT is only 5 nm; scale bar is 5 nm. (b) The outer walls of Ox-MWNT, after acid treatment at high temperature, show a high number of defects, indicative of carboxyl group functionalization on the outer surface; scale bar is 10 nm. (c) During the oxidation process, although Ox-MWNTs are shortened, the overall structure remains intact. (d) Cartoon depicting the oxidation process.

pellets using the GenElute Mammalian Total RNA Purification Kit (Sigma-Aldrich). Following DNase treatment, samples were heated at 70 °C for 10 min to inactivate DNase and RNase, and then chilled on ice. The amount of total RNA was determined at 260 nm using the NanoDrop 2000/2000c spectrophotometer (Thermo-Fisher Scientific), and the purity using the ratio of absorbance at 260/280 nm ratio. The cDNA was synthesized using High Capacity RNA to cDNA Kit (Applied Biosystems) using 2 µg of total RNA extract.

Primer sequences, designed and analyzed for specificity via <http://blast.ncbi.nlm.nih.gov/Blast.cgi>, included: 18S forward (5'-ATGGCCGTTCTTAGTTGGTG-3'), 18S reverse (5'-CGCTGAGCCAGTCAGTGTAG-3'); IL-1β forward (5'-GGA CAAGCTGAGGAAGATGC-3'), IL-1β reverse (5'-TCGTTATCC CATGTGTCGAA-3'); IL-6 forward (5'-GAAAGCAGCAAA GAGGCACT-3'), IL-6 reverse (5'-TTTCACCAGGC AAGTCTCCT-3'); IL-10 forward (5'-TTACCTGGAGGAGGTG ATGC-3'), IL-10 reverse (5'-GGCCTTGCTCTTGTTTTCAC-3'); IL-12 forward (5'-AACTTGACAGCTGAAGCCATT-3'), IL-12 reverse (5'-GACCTGAACGCAGAATGTCA-3'); TGF-β forward (5'-GTACCTGAACCCGTGTTGCT-3'), TGF-β reverse (5'-G TATCGCCAGGAATTGTTGC-3'); TNF-α forward (5'-AGCCC ATGTTGTAGCAAACC-3'), TNF-α reverse (5'-TGAGGTACA GGCCCTCTGAT-3'); NF-κB forward (5'-GTATTCAACCACA GATGGCACT-3'), NF-κB reverse (5'-AACCTTTGCTGGTCCCA CAT-3'); NLRP3 forward (5'-GCCATTCCTGACCAGACTC-3') and NLRP3 reverse (5'-GCAGGTAAAGGTGCGTGAGA-3').

The qPCR reaction (10 µl) consisted of 5 µl Power SYBR Green MasterMix (ABI), 75 nM of forward and reverse primer

and 500 ng template cDNA. PCR was performed using a Step One Plus Real-Time PCR System (ABI). After initiation steps of 2 min at 50 °C and 10 min at 95 °C, the template was amplified for 40 cycles (15 s at 95 °C, 1 min at 60 °C). Samples were normalized using the expression of human 18S rRNA. Data were analyzed using the Step One software v2.3. Ct (cycle threshold) values for each cytokine target gene were calculated. Relative expression of each cytokine target gene was calculated using the Relative Quantification (RQ) value, using the equation: $RQ = 2^{-\Delta\Delta Ct}$ for each cytokine target gene, and comparing relative expression with that of the 18S rRNA constitutive gene product. Assays were conducted in triplicate.

Multiplex cytokine array analysis

Cytokines (IL-6, IL-8, IL-10, IL12p40, IL12p70, IL-23, IL-27, IL-1α and IL-1β) and chemokines/growth factors (MIG, I-TAC, MCP-1, G-CSF and M-CSF) concentrations in the supernatants of U937 cells were measured by MagPix Milliplex kit (EMD Millipore). Cells were incubated with protein-coated and uncoated CMC-MWNTs and Ox-MWNTs as above for 48 h, and then spun down at 300g and supernatants were stored at -80 °C until use. Briefly, 25 µl of assay buffer was added to each well of a 96-well plate, followed by addition of 25 µl of standard, controls or supernatants of (CNT treated) cells, to appropriate wells. Twenty-five microliters of magnetic beads coupled to analytes was added in each well, and incubated for 18 h at 4 °C. After washing the plate with assay buffer, 25 µl of detection antibodies was incubated with the beads for 1 h at RT.

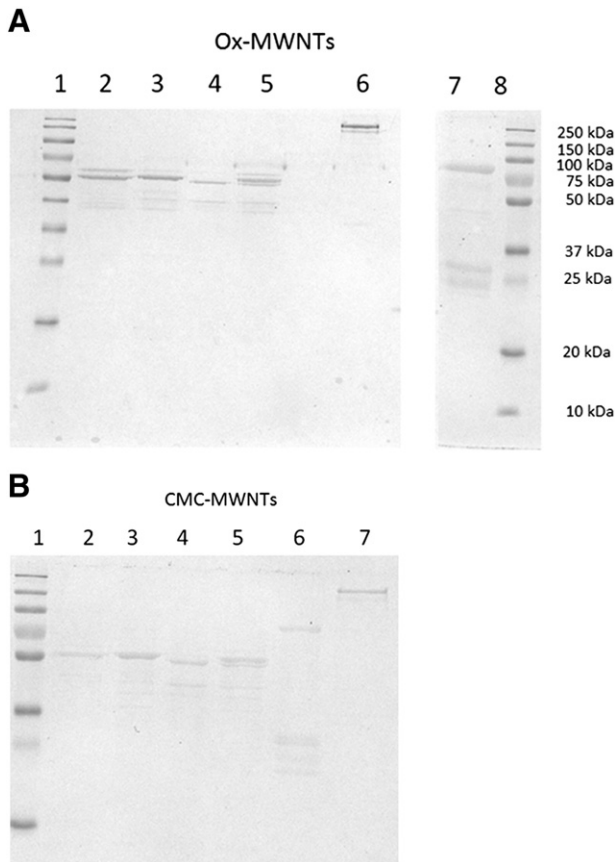


Figure 2. (A) SDS-PAGE of purified proteins bound to Ox-MWNTs. CNTs were coated with the proteins (1:2 ratio) for 2 h. Lane 1: standard marker; Lanes 2, 3 and 4 containing: ghA, ghB and ghC, respectively (each ~60 kDa); Lane 5: equimolar ghA, ghB and ghC; Lane 6: factor H (~155 kDa); Lane 7: C1q (A, B, and C chains at ~20–25 kDa); Lane 8: marker. (B) SDS-PAGE of purified proteins bound to CMC-CNTs. CNTs were coated with the proteins as above Lane 1: molecular weight marker; Lane 2: ghA; Lane 3: ghB; Lane 4: ghC; Lane 5: equimolar ghA, ghB and ghC; Lane 6: C1q; Lane 7: factor H. In Fig. 2, A and B, the additional band in the C1q tracks (above 70 kDa) may arise from aggregation of C1q C chain, or incomplete dissociation of C1q.

Twenty-five microliters of streptavidin–phycoerythrin was then added and incubated for 30'. Following a washing step, 150 μ l of sheath fluid (BD Biosciences) was added to each well and the plate was read using the Luminex Magpix instrument.

Results

Oxidation, coating and dispersion of CNTs

Pristine MWNTs of 5–20 μ m length and a diameter of 10–20 nm (Figure 1, A) were well-dispersed by non-covalent coating with CMC; being stable over months, no sedimentation/clustering is seen (by light microscopy; not shown). Oxidation was achieved by treatment with concentrated acids (Figure 1, D). Defects seen on the surface of the Ox-MWNTs via TEM imaging (Figure 1, B) were absent on pristine MWNTs (Figure 1, A); CNTs were significantly shortened (length 100–500 nm; Figure 1, C). NaOH treatment removed all amorphous carbon from the CNT

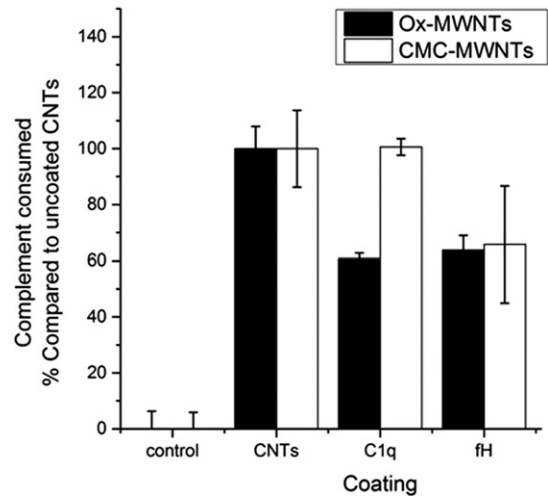


Figure 3. Complement consumption assay. CNTs were coated with the proteins (1:4 ratio) overnight and washed, followed by incubation with human serum for 1 h. Serum incubated without CNTs acted as a negative control. % complement consumption was calculated as $(C - C_i)/C \times 100\%$, where C is total complement activity in CH50 units of the negative control, C_i the amount of activity remaining in the supernatant. All experiments were done in triplicate; error bars represent \pm standard deviation.

surface. Ox-MWNTs were stable over months even at >1 mg/ml without clustering/sedimentation.

Binding of wild type and substitution mutants of individual C1q globular domains to CNTs suggests a charge–charge interaction

C1q and FH both bound to CMC-MWNTs and Ox-MWNTs (Figure 2, A, B; lanes 6, 7). Differential binding of ghA, ghB and ghC and their mutants can be seen in Supplementary Figure 1. For Ox-MWNT, binding of ghA and ghB was stronger than ghC (Figure 2, A; lanes 2–5). For CMC-MWNT, binding of ghB was stronger than ghA and ghC (Figure 2, B; lanes 2–5). Arg^{A162} appeared important since binding decreased for Arg^{A162}Ala, while wild-type and Arg^{A162}Glu bound similarly (Supplementary Figure 1, A and B). Substitution of Lys136 to Glu (Lys^{B136}Glu) abolished binding completely. Furthermore, Arg^{B129} substitution had a negative effect. When Arg129 was substituted for Ala, a decrease in binding was observed, while substitution for Glu did not have an effect. No other ghB substitutions (Arg^{B114}Gln/Glu, His^{B117}Asp, Arg^{B163}Ala/Glu, Tyr^{B175}Leu) had a large influence on binding. For ghC, mutants His^{C101}Ala and Lys^{C170}Glu did not have an effect on binding; however, Arg^{C156}Glu showed an increase in binding. Thus, C1q binds to CNT surface patterns in a manner different from its natural ligands, especially IgG and IgM. Residues that have previously shown to be peripheral and subsidiary for gC1q interaction with natural ligands seem important for interaction with CNTs.

Coating of CNTs with innate immune humoral factors and effect on classical pathway complement activation

When C1q-coated Ox-MWNT and CMC-MWNT were examined for the classical pathway activation, complement consumption was inhibited by 40% for Ox-MWNTs but there

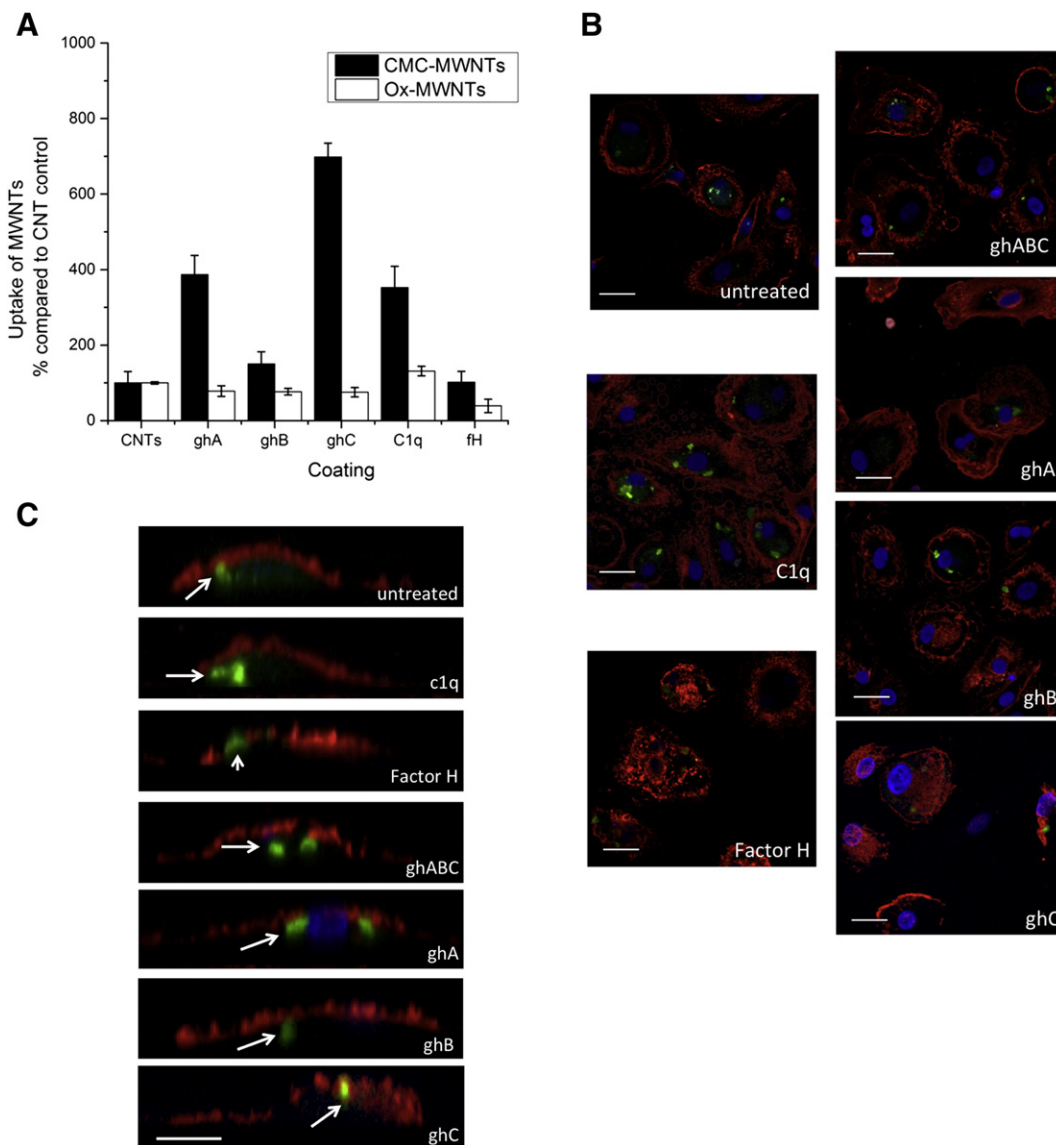


Figure 4. Differential phagocytosis by macrophages of CMC-CNTs coated with C1q, factor H, ghA, ghB and ghC. (A) 0.5×10^6 U937 cells were incubated with $20 \mu\text{g}$ of protein-coated biotin-CNTs for 6 h. The cells were lysed and the amount of CNTs was quantified by an ELISA type assay. A standard curve with known concentrations of biotin-CMC-CNTs was performed in the same assay to calculate the mass of the CNTs in the cell samples. All experiments were done in triplicate; error bars represent \pm standard deviation. (B) *In vitro* assessment of uptake of protein-treated and untreated fluorescently labeled CMC-MWNTs by human blood macrophages. Cells were incubated for 3 h with Alexa 488 cadaverine labeled-CMC-MWNTs (green) pre-incubated with C1q, factor H, ghA, ghB or ghC, or a mix (ghABC). Cells were fixed and stained with Alexa546-labeled WGA to reveal the plasma membrane (red). The nucleus was stained with Hoechst 33342 (blue). Single confocal sections are shown, scale bars $20 \mu\text{m}$. (C) Magnified orthogonal views of the same confocal images demonstrate uptake of Alexa 488 cadaverine labeled-CMC-MWNTs (green, arrows) for all proteins but factor H (small arrow), scale bar $10 \mu\text{m}$.

was no inhibition for CMC-MWNT (Figure 3), suggesting differential orientation of C1q on the CNT surface. CNT-bound C1q must either sequester C1r and C1s from C1 in the serum, or be replaced by C1. Since ghA, ghB and ghC do not apparently dissociate (see below), the interaction of C1q with Ox-MWNT may be at least partially in a conformation which does not allow capture of C1r and C1s. Coating with ghA, ghB and ghC also considerably inhibits the classical pathway activation by serum.²¹ CNTs, when pre-coated with FH (Figure 3), were also able to consume 40% less complement than the uncoated CNTs. This indicates that FH is inhibiting binding of C1 (C1q)

from serum, possibly recognizing motifs that are overlapping/identical to those recognized by C1q, consistent with the emerging evidence that for certain C1q ligands, such as anionic phospholipids, lipid A, apoptotic cells and β amyloid peptide 1-42, FH can be an inhibitor of the classical pathway.^{11,13,24,30}

Effect of CNT coating with C1q, ghA, ghB, ghC and factor H on phagocytosis by U937 cell line and human macrophages

For CMC-MWNT, phagocytosis was increased by C1q (3.5-fold), ghA (4-fold), and ghC (7-fold) (Figure 4, A). For Ox-MWNT, no

significant effect was seen for any of the globular head modules, but phagocytosis was slightly higher with C1q (1.3 fold). For FH, a 2.6 fold reduction of uptake of Ox-MWNT was seen, but FH did not enhance or diminish uptake of CMC-MWNT. The enhancement of CMC-MWNT uptake by individual gC1q modules is novel and curious. Confocal microscopy using human macrophages confirmed that C1q and the recombinant gC1q modules, but not FH, enhanced uptake of CMC-MWNTs (Figure 4, B). Single confocal sections with higher magnification of the membrane revealed qualitative localization of CNTs inside the cells except in the case of FH (Figure 4, C).

Cytokine and transcription factor mRNA expression by U937 cells treated with protein-coated Ox-MWNTs and CMC-MWNTs

IL-10 mRNA expression by U937 cells was dramatically up-regulated (300-fold by 6 h) by Ox-MWNT from 15 min onwards (Supplementary Figure 2); for CMC-MWNT, the up-regulation was seen only after 2 h. For Ox-MWNT, pre-coating with C1q and ghC dampened the IL-10 expression compared to uncoated Ox-MWNTs. For CMC-MWNTs, all proteins except FH had an inhibitory effect on IL-10, ghC being the most pronounced. IL-12 transcription was considerably up-regulated for Ox-MWNTs by ghA, ghB and ghC, but not as much as by C1q and FH. IL-12 expression was down-regulated by CMC-MWNT on its own, and further dampened by FH. For Ox-MWNTs, TGF- β was down-regulated by C1q, but overall up-regulated by FH, ghB and ghC, suggesting an immunosuppressive effect. However, for CMC-MWNT, C1q and gC1q modules up-regulated TGF- β transcripts while FH down-regulated, suggesting pattern-dependent modulation of anti-inflammatory response. IL-1 β was up-regulated for all Ox-MWNT; for CMC-MWNT, there was initially a down-regulation of IL-1 β , but it increased at 2 h and 3 h, consistent with NLRP3 expression. For IL-6, CMC-CNT (uncoated) caused a consistently moderate down-regulation, which was generally reversed by coating with C1q, FH, ghA, ghB and ghC. TNF- α was up-regulated by Ox-MWNTs; most proteins induced up-regulation at various time points, consistent with NF- κ B expression profile (Supplementary Figure 2).

Modulatory effects of protein-coated CNTs on cytokine/chemokine secretion by U937 cells

Cytokine array analysis using supernatants at 48 h from experiments as in Supplementary Figure 2 revealed that FH suppressed MCP-1, IL-8 and TNF- α (FH more pronounced for Ox-MWNT), IL-10, IL-1 α and IL-1 β . C1q, as opposed to FH, enhanced TNF- β , IL-1 β , IL-10 and G-CSF secretion. All three globular modules suppressed IL-8 and G-CSF, while TNF- α was suppressed by ghB and ghC. IL-10 secretion was slightly enhanced whereas ghB considerably suppressed IL-1 α and IL-1 β for CMC-MWNT. They also enhanced G-CSF production whereas only ghA was able to enhance IL-12 secretion (Figure 5).

Discussion

Due to a range of structural and functional attributes, CNTs have wide ranging applications in translational medicine.^{31–35} Their systemic administration for vaccination and drug delivery^{31,34,36}

inevitably brings them in contact with complement. Any surface that offers a molecular pattern as a signature of non-self and altered-self is amenable to complement recognition and activation. Complement deposition on CNTs, mainly via the classical pathway,^{3,6,17,21} enhances their uptake by complement receptor bearing APCs such as macrophages and B cells and down-regulates pro-inflammatory cytokines²¹ via up-regulation of IL-10.²² Curiously, Au–Ni nanowires,^{22,37} being poor complement activators, are potent inducers of pro-inflammatory response following serum treatment, suggesting that coating with other serum proteins in the absence of complement deposition can have deleterious consequences.²² This brought the focus of this study on the nature of the interaction between C1q⁹ and CNTs.

All three recombinant globular head modules (ghA, ghB, ghC) bind onto the surface indicating the binding of C1q onto CNTs is likely through charge pattern recognition, which would enable binding of C1r and C1s via C1q for further complement activation. Coating the globular heads lead to effective inhibition of complement activation.²¹ We used single residue substitute mutations of ghA, ghB and ghC in order to identify gC1q residues involved in the CNT–C1q interaction. These residues were selected for substitution mutation because of being hypervariable within the 3-D structure of the gC1q domain and their central/subsidiary involvement in interaction with known C1q ligands.^{27–29,38} We also examined the effects of CNT coating by C1q, ghA, ghB, ghC, and FH (as a potential down-regulator of the classical pathway) on phagocytosis and cytokine expression by macrophages. Salvador-Morales et al⁸ have shown that FH reduces complement activation by CNTs through the alternative pathway. For a number of C1q ligands, FH acts an inhibitor of C1q, and thus dampens the classical pathway.^{11,13,24,30} C1q and FH can be locally synthesized in tissues, and thus bind to CNTs and alter their interaction with immune cells without involving complement activation.

C1q is a versatile pattern recognition innate immune molecule that recognizes an array of self, non-self and altered-self ligands. The broad-spectrum ligand-binding potential of C1q, and its subsequent effect on biological processes, is facilitated by the modular organisation of the heterotrimeric gC1q domain (where each module can have independence of structure and function), its ability to change its conformation in a very subtle way, and the manner in which this ancient molecule has evolved.^{9,38–40} The versatility and variability of C1q–ligand interaction are due to differences in electrostatic surface potentials of the different gC1q modules.⁴¹ Substitution mutants used here were designed based on structure–function studies and ConSurf⁴² where the most variable residues in the C1q family were considered most likely to be central to C1q–ligand interaction. Thus, Arg^{B114} and Arg^{B129}, known to be important for C1q–IgG interaction²⁷ did not seem crucial for CNTs. Interestingly, an increase of binding was found for substitution of the Arg^{C156} to Glu. These results appear to suggest involvement of side chains and hydrophobic patches within the gC1q domain in their interaction with CNTs. Binding of macromolecules on CNTs is not fully explored, but may involve charge transfer and hydrophobic interaction.^{43,44} Thus, molecular patterns offered by CNTs are likely to act as a nucleation centre for an ordered binding of C1q and FH. Here, residues within the gC1q domain that are peripheral/subsidiary to

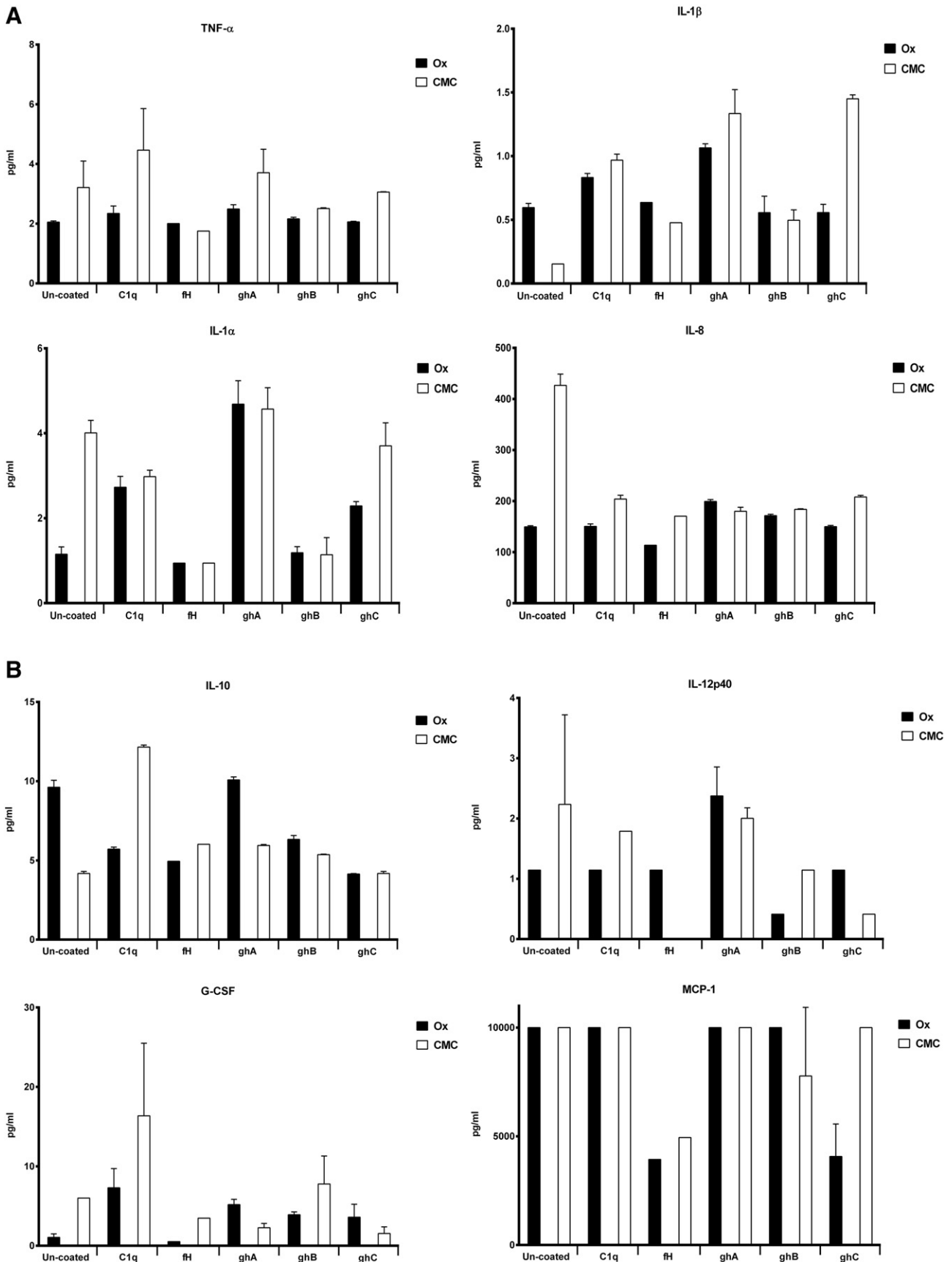


Figure 5. Multiplex cytokine array analysis of supernatants of U937 cells treated with Ox-MWNT and CMC-CNT coated or uncoated with proteins for 24 h.

C1q binding with its known natural ligands appeared to be involved in C1q-CNT interaction. These molecular patterns may impact upon the level of C1q binding to CNTs, their clearance by phagocytic cells, and cellular toxicity.

Oxidized CNTs are in general considered less toxic than pristine CNTs.^{45–51} These effects, and few disagreements, are due to reduction of impurities (catalyst) in the samples, a decrease in length of CNTs, an increase of functional groups, and higher dispersability leading to higher bioavailability.^{52,53} Bio-persistence is an important parameter for nanoparticle *in vivo* toxicity. In contrast to pristine CNTs, highly carboxylated CNTs were shown to be rapidly (within 3 h) cleared out of the systematic circulation through the renal excretion route.⁴⁸ Possible enzymatic degradation of CNTs with HRP^{49,54} and myeloperoxidase (expressed in neutrophils)⁵⁵ can thus be avoided since CNT oxidation reduces the time required for degradation.^{49,56} Thus, coating and downstream processing of CNTs can generate new molecular signatures that can be recognized by complement proteins including C1q.

The dissection of C1q interaction with CNTs is insightful given that C1q is capable of binding charge clusters, polar regions, or small hydrophobic patches.³⁸ Since CNTs offer repetitive patterns of polarity and hydrophobicity, C1q is well suited to bind them, activate the classical pathway, and also enhance their phagocytic uptake directly, even without further complement deposition. Here, we report that coating CNTs with recombinant globular heads can inhibit the classical pathway activation, enhance uptake of CNTs by phagocytic cells, and at the same time down-regulate pro-inflammatory cytokine response by macrophages: a very novel and surprising result since these molecules lack the collagen region of human C1q, which is generally thought to be implicated in binding to receptors involved in phagocytosis. However, there is at least one putative receptor, gC1qR which recognizes globular heads.²⁵ Thus, the mechanism of enhancement of CNT uptake by globular heads of C1q needs to be examined in future studies. We report a novel method of inhibition of nanoparticle-mediated activation of the classical pathway and subsequent handling by phagocytic cells through an anti-inflammatory route. In view of planned trials using CNTs coated with therapeutic antibodies^{35,57–60} which are likely to offer an array of closely spaced Fc regions for C1q to bind, the study offers an opportunity to modify drug vehicles.

Appendix A. Supplementary data

Supplementary data to this article can be found online at <http://dx.doi.org/10.1016/j.nano.2015.06.009>.

References

- Hussain S, Vanoirbeek JAJ, Hoet PHM. Interactions of nanomaterials with the immune system. *Wiley Interdiscip Rev Nanomed Nanobiotechnol* 2012;**4**:169–83.
- Zolnik BS, Gonzalez-Fernandez A, Sadrieh N, Dobrovolskaia MA. Minireview: nanoparticles and the immune system. *Endocrinology* 2010;**151**:458–65.
- Rybak-Smith M, Pondman K, Flahaut E, Salvador-Morales C, Sim R. Recognition of carbon nanotubes by the human innate immune system. In: Klingeler R, Sim RB, editors. *Carbon Nanotub. Biomed. Appl.* Springer; 2011. p. 183–210.
- Andersen AJ, Wibroe PP, Moghimi SM. Perspectives on carbon nanotube-mediated adverse immune effects. *Adv Drug Deliv Rev* 2012;**64**:1700–5.
- Dumortier H. When carbon nanotubes encounter the immune system: desirable and undesirable effects. *Adv Drug Deliv Rev* 2013;**65**:2120–6.
- Salvador-Morales C, Flahaut E, Sim E, Sloan J, Green ML, Sim RB. Complement activation and protein adsorption by carbon nanotubes. *Mol Immunol* 2006;**43**:193–201.
- Salvador-Morales C, Townsend P, Flahaut E, Venien-Bryan C, Vlandas A, Green MLH, et al. Binding of pulmonary surfactant proteins to carbon nanotubes; potential for damage to lung immune defense mechanisms. *Carbon* 2007;**45**:607–17.
- Salvador-Morales C, Basiuk EV, Basiuk VA, Green MLH, Sim RB. Effects of covalent functionalization on the biocompatibility characteristics of multi-walled carbon nanotubes. *J Nanosci Nanotechnol* 2008;**8**:2347–56.
- Kishore U, Reid KB. Modular organization of proteins containing C1q-like globular domain. *Immunopharmacology* 1999;**42**:15–21.
- Carroll MV, Sim RB. Complement in health and disease. *Adv Drug Deliv Rev* 2011;**63**:965–75.
- Kishore U, Sim RB. Factor H as a regulator of the classical pathway activation. *Immunobiology* 2012;**217**:162–8.
- Kouser L, Abdul-Aziz M, Nayak A, Stover CM, Sim RB, Kishore U. Properdin and factor H: opposing players on the alternative complement pathway “see-saw”. *Front Immunol* 2013;**4**:93.
- Tan LA, Yu B, Sim FCJ, Kishore U, Sim RB. Complement activation by phospholipids: the interplay of factor H and C1q. *Protein Cell* 2010;**1**:1033–49.
- Hamad I, Hunter AC, Rutt KJ, Liu Z, Dai H, Moghimi SM. Complement activation by PEGylated single-walled carbon nanotubes is independent of C1q and alternative pathway turnover. *Mol Immunol* 2008;**45**:3797–803.
- Moghimi SM, Hunter AC. Complement monitoring of carbon nanotubes. *Nat Nanotechnol* 2010;**5**:382 [author reply 382–3].
- Ling WL, Biro A, Bally I, Tacnet P, Deniaud A, Doris E, et al. Proteins of the innate immune system crystallize on carbon nanotubes but are not activated. *ACS Nano* 2011;**5**:730–7.
- Rybak-Smith MJ, Sim RB. Complement activation by carbon nanotubes. *Adv Drug Deliv Rev* 2011;**63**:1031–41.
- Rybak-Smith MJ, Tripisciano C, Borowiak-Palen E, Lamprecht C, Sim RB. Effect of functionalization of carbon nanotubes with psychosine on complement activation and protein adsorption. *J Biomed Nanotechnol* 2011;**7**:830–9.
- Andersen AJ, Robinson JT, Dai HJ, Hunter AC, Andresen TL, Moghimi SM. Single-walled carbon nanotube surface control of complement recognition and activation. *ACS Nano* 2013;**7**:1108–19.
- Andersen AJ, Windschiegl B, Ilbasnis-Tamer S, Degim IT, Hunter AC, Andresen TL, et al. Complement activation by PEG-functionalized multi-walled carbon nanotubes is independent of PEG molecular mass and surface density. *Nanomedicine* 2013;**9**:469–73.
- Pondman KM, Sobik M, Nayak A, Tsolaki AG, Jäkel A, Flahaut E, et al. Complement activation by carbon nanotubes and its influence on the phagocytosis and cytokine response by macrophages. *Nanomedicine* 2014;**10**:1287–99.
- Pondman KM, Tsolaki AG, Paudal B, Shamji MH, Switzer A, Pathan AA, et al. Complement deposition on nanoparticles can modulate immune responses by macrophage, B and T cells. *J Biomed Nanotechnol* 2015 [in press].
- Li Y, Zhang X, Luo J, Huang W, Cheng J, Luo Z, et al. Purification of CVD synthesized single-wall carbon nanotubes by different acid oxidation treatments. *Nanotechnology* 2004;**15**:1645–9.
- Tan LA, Yang AC, Kishore U, Sim RB. Interactions of complement proteins C1q and factor H with lipid A and *Escherichia coli*: further

- evidence that factor H regulates the classical complement pathway. *Protein Cell* 2011;**2**:320-32.
25. Kouser L, Madhukaran SP, Shastri A, Saraon A, Ferluga J, Al-Mozaini M, et al. Emerging and novel functions of complement protein C1q. *Front Immunol* 2015;**6**:317.
 26. Verdejo R, Lamoriniere S, Cottam B, Bismarck A, Shaffer M. Removal of oxidation debris from multi-walled carbon nanotubes. *Chem Commun* 2007;**5**:13-5.
 27. Kojouharova MS, Gadjeva MG, Tsacheva IG, Zlatarova A, Roumenina LT, Tchorbadjieva MI, et al. Mutational analyses of the recombinant globular regions of human C1q A, B, and C chains suggest an essential role for arginine and histidine residues in the C1q-IgG interaction. *J Immunol* 2004;**172**:4351-8.
 28. Roumenina LT, Ruseva MM, Zlatarova A, Ghai R, Kolev M, Olova N, et al. Interaction of C1q with IgG1, C-reactive protein and pentraxin 3: mutational studies using recombinant globular head modules of human C1q A, B, and C chains. *Biochemistry* 2006;**45**:4093-104.
 29. Gadjeva MG, Rouseva MM, Zlatarova AS, Reid KBM, Kishore U, Kojouharova MS. Interaction of human C1q with IgG and IgM: revisited. *Biochemistry* 2008;**47**:13093-102.
 30. Kang Y-H, Urban BC, Sim RB, Kishore U. Human complement Factor H modulates C1q-mediated phagocytosis of apoptotic cells. *Immunobiology* 2012;**217**:455-64.
 31. Bianco A, Kostarelos K, Prato M. Applications of carbon nanotubes in drug delivery. *Curr Opin Chem Biol* 2005;**9**:674-9.
 32. Li JG, Li WX, Xu JY, Cai XQ, Liu RL, Li YJ, et al. Comparative study of pathological lesions induced by multiwalled carbon nanotubes in lungs of mice by intratracheal instillation and inhalation. *Environ Toxicol* 2007;**22**:415-21.
 33. Shi XF, Sitharaman B, Pham QP, Liang F, Wu K, Billups WE, et al. Fabrication of porous ultra-short single-walled carbon nanotube nanocomposite scaffolds for bone tissue engineering. *Biomaterials* 2007;**28**:4078-90.
 34. Ali-Boucetta H, Al-Jamal KT, McCarthy D, Prato M, Bianco A, Kostarelos K. Multiwalled carbon nanotube-doxorubicin supramolecular complexes for cancer therapeutics. *Chem Commun* 2008:459-61.
 35. Heister E, Neves V, Tilmaciu C, Lipert K, Beltrán VS, Coley HM, et al. Triple functionalisation of single-walled carbon nanotubes with doxorubicin, a monoclonal antibody, and a fluorescent marker for targeted cancer therapy. *Carbon* 2009;**47**:2152-60.
 36. Pantarotto D, Partidos CD, Hoebeke J, Brown F, Kramer E, Briand J-P, et al. Immunization with peptide-functionalized carbon nanotubes enhances virus-specific neutralizing antibody responses. *Chem Biol* 2003;**10**:961-6.
 37. Pondman KM, Maijenburg AW, Celikkol FB, Pathan AA, Kishore U, ten Haken B, et al. Au coated Ni nanowires with tuneable dimensions for biomedical applications. *J Mater Chem B* 2013;**1**:6129-36.
 38. Kishore U, Ghai R, Greenhough TJ, Shrive AK, Bonifati DM, Gadjeva MG, et al. Structural and functional anatomy of the globular domain of complement protein C1q. *Immunol Lett* 2004;**95**:113-28.
 39. Sim RB, Reid KB. C1: molecular interactions with activating systems. *Immunol Today* 1991;**12**:307-11.
 40. Kishore U, Gupta SK, Perdikoulis MV, Kojouharova MS, Urban BC, Reid KBM. Modular organization of the carboxyl-terminal, globular head region of human C1q A, B, and C chains. *J Immunol* 2003;**171**:812-20.
 41. Gaboriaud C, Juanhuix J, Gruez A, Lacroix M, Damault C, Pignol D, et al. The crystal structure of the globular head of complement protein C1q provides a basis for its versatile recognition properties. *J Biol Chem* 2003;**278**:46974-82.
 42. Ghai R, Waters P, Roumenina LT, Gadjeva M, Kojouharova MS, Reid KBM, et al. C1q and its growing family. *Immunobiology* 2007;**212**:253-66.
 43. Balavoine F, Schultz P, Richard C, Mallouh V, Ebbesen TW, Mioskowski C. Helical crystallization of proteins on carbon nanotubes: a first step towards the development of new biosensors. *Angew Chem Int Ed Engl* 1999;**38**:1912-5.
 44. Pan B, Xing B. Adsorption mechanisms of organic chemicals on carbon nanotubes. *Environ Sci Technol* 2008;**42**:9005-13.
 45. Pulskamp K, Diabaté S, Krug HF. Carbon nanotubes show no sign of acute toxicity but induce intracellular reactive oxygen species in dependence on contaminants. *Toxicol Lett* 2007;**168**:58-74.
 46. Ji Z, Zhang D, Li L, Shen X, Deng X, Dong L, et al. The hepatotoxicity of multi-walled carbon nanotubes in mice. *Nanotechnology* 2009;**20**:445101.
 47. Boncel S, Muller KH, Skepper JN, Walczak KZ, Koziol KK. Tunable chemistry and morphology of multi-wall carbon nanotubes as a route to non-toxic, theranostic systems. *Biomaterials* 2011;**32**:7677-86.
 48. Jain S, Thakare VS, Das M, Godugu C, Jain AK, Mathur R, et al. Toxicity of multiwalled carbon nanotubes with end defects critically depends on their functionalization density. *Chem Res Toxicol* 2011;**24**:2028-39.
 49. Zhao Y, Allen BL, Star A. Enzymatic degradation of multiwalled carbon nanotubes. *J Phys Chem A* 2011;**115**:9536-44.
 50. Muller J, Huaux F, Fonseca A, Nagy JB, Moreau N, Delos M, et al. Structural defects play a major role in the acute lung toxicity of multiwall carbon nanotubes: toxicological aspects. *Chem Res Toxicol* 2008;**21**:1698-705.
 51. Singh RP, Das M, Thakare V, Jain S. Functionalization density dependent toxicity of oxidized multiwalled carbon nanotubes in a murine macrophage cell line. *Chem Res Toxicol* 2012;**25**:2127-37.
 52. Wick P, Manser P, Limbach LK, Dettlaff-Weglikowska U, Krumeich F, Roth S, et al. The degree and kind of agglomeration affect carbon nanotube cytotoxicity. *Toxicol Lett* 2007;**168**:121-31.
 53. Heister E, Lamprecht C, Neves V, Tilmaciu C. Higher dispersion efficacy of functionalized carbon nanotubes in chemical and biological environments. *ACS Nano* 2010;**4**:2615-26.
 54. Liu X, Hurt RH, Kane AB. Biodurability of single-walled carbon nanotubes depends on surface functionalization. *Carbon* 2010;**48**:1961-9.
 55. Kagan VE, Konduru NV, Feng W, Allen BL, Conroy J, Volkov Y, et al. Carbon nanotubes degraded by neutrophil myeloperoxidase induce less pulmonary inflammation. *Nat Nanotechnol* 2010;**5**:354-9.
 56. Russier J, Ménard-Moyon C, Venturelli E, Gravel E, Marcolongo G, Meneghetti M, et al. Oxidative biodegradation of single- and multi-walled carbon nanotubes. *Nanoscale* 2011;**3**:893-6.
 57. McDevitt MR, Chattopadhyay D, Kappel BJ, Jaggi JS, Schiffman SR, Antezak C, et al. Tumor targeting with antibody-functionalized, radiolabeled carbon nanotubes. *J Nucl Med* 2007;**48**:1180-9.
 58. Xiao Y, Gao X, Taratula O, Treado S, Urbas A, Holbrook RD, et al. Anti-HER2 IgY antibody-functionalized single-walled carbon nanotubes for detection and selective destruction of breast cancer cells. *BMC Cancer* 2009;**9**:351.
 59. Cardoso MM, Peca IN, Roque ACA. Antibody-conjugated nanoparticles for therapeutic applications. *Curr Med Chem* 2012;**19**:3103-27.
 60. Lee IH, Lee JM, Jung Y. Controlled protein embedding onto Au/Ag core-shell nanoparticles for immuno-labeling of nanosilver surface. *ACS Appl Mater Interfaces* 2014;**6**:7659-64.